

A novel anticancer agent, icaritin, induced cell growth inhibition, G₁ arrest and mitochondrial transmembrane potential drop in human prostate carcinoma PC-3 cells[☆]

Xin Huang¹, Danyan Zhu¹, Yijia Lou^{*}

Institute of Pharmacology & Toxicology and Biochemical Pharmaceutics, College of Pharmaceutical Sciences, Zhejiang University, 353, Yan'an Road, Hangzhou, 310031, China

Received 2 June 2006; received in revised form 26 January 2007; accepted 1 February 2007
Available online 27 February 2007

Abstract

Icariin and icaritin with prenyl group have been demonstrated for their selective estrogen receptor modulating activities. We screened their effects on cell growth in human prostate carcinoma PC-3 cell line (estrogen receptor positive) *in vitro*. PC-3 cell line was used for the measurement of anti-carcinoma activities of 0–100 $\mu\text{mol/l}$ icaritin and 30 $\mu\text{mol/l}$ icariin. 1 $\mu\text{mol/l}$ 17- β estradiol (E₂) served as the estrogen positive control, and 1 $\mu\text{mol/l}$ ICI 182,780 [7 α -[9 (4,4,5,5,5-pentafluoropentyl) sulfinyl] nonyl]-estra-1,3,5(10)-triene-3,17 α -diol] served as the specific estrogen receptor antagonist. Primary cultured rat prostate basal cells used as cell growth selective control. The growth-inhibitory effects were analyzed using MTT assay, and fluorochrome staining, flow cytometry, and immunoblotting were employed to illustrate the possible mechanisms. When treated with icaritin for 24 to 72 h, cell growth was strongly inhibited (at 48 h IC₅₀ was 10.74 \pm 1.59 $\mu\text{mol/l}$, $P < 0.001$) accompanied with a mitochondrial transmembrane potential ($-\Psi_m$) drop. Meanwhile, few changes in IC₅₀ could be observed when co-incubated with ICI 182,780. Icaritin-induced growth inhibition was associated with G₁ arrest ($P < 0.05$), and G₂-M arrest depending upon doses. Consistently with G₁ arrest, icaritin increased protein expressions of pRb, p27^{Kip1} and p16^{Ink4a}, while showed decrease in phosphorylated pRb, Cyclin D1 and CDK4. Comparatively, icariin has much lower effects on PC-3 cells and showed only weak G₁ arrest, suggesting a possible structure–activity relationship. These findings suggested a novel anticancer efficacy of icaritin mediated selectively *via* induction of cell cycle arrest but not associated with estrogen receptors in PC-3 cells.

© 2007 Published by Elsevier B.V.

Keywords: Icaritin; Icariin; PC-3; G₁ arrest; Mitochondrial transmembrane potential ($-\Psi_m$); Apoptosis

1. Introduction

Prostate cancer is the most common cancer as well as the second leading cause of cancer-related deaths in men in Western countries (Greenlee et al., 2001). However, there has been a recent trend in Asia towards increasing incidence of prostate cancer, such as Japan and Singapore, reporting a more rapid increase than high-risk countries. Whilst the absolute value of

the increase is not comparable to North American and European populations, the incidence ratio in many Asian centers is similar to that of the high-risk countries (Sim and Cheng, 2005). At present, there is no effective therapy available for the treatment of androgen-independent stage of prostate cancer (advanced prostate cancer), which usually arises after hormonal deprivation/ablation therapy.

Naturally occurring icariin and icaritin present in *Epimedium brevicornum* Maxim. (Berberidaceae), which has been traditionally used in Chinese folk medicine that has a wide range of pharmacological and biological activities, including regulating cardiovascular, circulatory, genital, and bone marrow systems, stimulating neurite growth and possessing estrogenic activity (Wang and Lou, 2004; Liu and Lou, 2004; Ye and Lou, 2005). *In vitro* studies have demonstrated that icariin possesses

[☆] Grant sponsor: National Natural Science Foundation of China; Grant number: No. 30070904, 30171121, 30472112, 30672564.

^{*} Corresponding author. Tel./fax: +86 571 87217206.

E-mail addresses: hx06@yahoo.com.cn (X. Huang), zdyzxb@zju.edu.cn (D. Zhu), yijialou@zju.edu.cn (Y. Lou).

¹ Tel./fax: +86 571 87217206.

antitumor activity (Zhao et al., 1997), while icaritin exhibits its selective estrogen receptor modulating (SERM) effect mostly *via* estrogen receptor-related mediating pathway, acting as a phytoestrogen (Wang and Lou, 2004; Wang et al., 2006). Limited *in vitro* studies indicated that several prenylated flavonoids present in the hop plant (*Humulus lupulus*) possess anticarcinogenic properties (Colgate et al., 2006). Here, a prenylflavonoid named icaritin ($C_{20}H_{20}O_6$; molecular weight 356.38) and its glycoside icariin ($C_{33}H_{40}O_{15}$; molecular weight 676.65; which substituted Rha- and Glc-side chain for 3, 7-OH of icaritin]) (Fig. 1) were employed to find their anti-prostate carcinoma activities.

The phytoestrogens (flavonoids coumestans and lignans) may display estrogenic or anti-estrogenic activity by binding to the various forms of the estrogen receptor or by competing for the binding sites of estrogen biosynthesizing or metabolizing enzymes (Santti et al., 1998). It has been suggested that estrogens and their receptors may be involved in the development and progression of prostate cancer. Both estrogen α receptor and estrogen β receptor could be detected in the development of prostate cancer cell lines, such as LNCaP, DU145, and PC-3, and it appears unlikely that alterations in the expression of either estrogen receptor are commonly involved in the progression of prostate cancer. There is a higher affinity of phytoestrogens typically for estrogen β receptor than estrogen α receptor, and estrogen β receptor is expressed in the PC-3 prostate epithelial cell lines *in vitro* (Linja et al., 2003).

However, there is no report on the evaluation of anticancer activity of the selective estrogen receptor modulators, icaritin and icariin against prostate cancers. In the present investigation, human prostate carcinoma PC-3 cells were employed to evaluate the anticancer activity of icariin and icaritin, and for the first time tested their efficacy against human prostate carcinoma PC-3 cells. We hypothesized there exists a structure–activity relationship inside these compounds by showing their efficacy in inhibiting growth and causing death of PC-3 cells. Furthermore, we investigated the mechanistic rationale for the observed efficacy of these compounds and hope those could be the most likely targets for clinical therapy in prostate cancer cells.

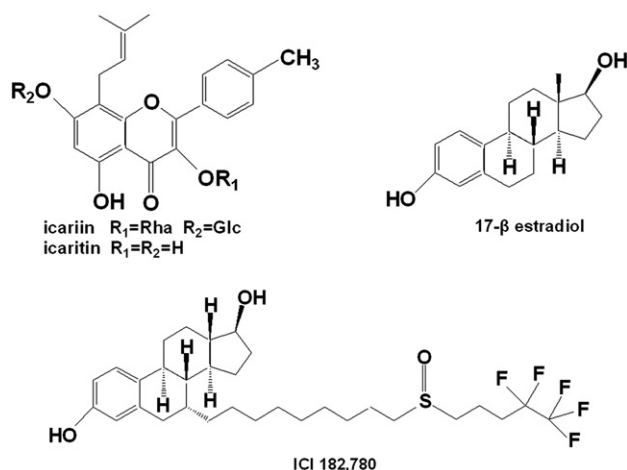


Fig. 1. Chemical structures of icariin, icaritin, 17- β estradiol, and ICI 182,780.

2. Materials and methods

2.1. Preparation for icariin and icaritin

Icariin was purchased from Zhejiang institute for the control of pharmaceutical and biological products. Its hydrolysate, icaritin, was prepared from icariin by treatment with cellulase enzyme and purified using High Performance Liquid Chromatography (HPLC) method. The structure of icaritin was determined by mass spectrometry (esquire300plus_01073) analysis. These compounds were dissolved in dimethyl sulphoxide (DMSO) as stock solutions, and used directly in the cell culture treatment.

2.2. Cell lines and cell growth-inhibition studies

The human prostate cancer cell line PC-3 was obtained from Institute of Biochemistry and Cell Biology, SIBS, CAS and cultured in RPMI 1640 medium (Gibco, Rockville, MD, USA), supplemented with 10% bovine serum albumin (BSA), 1% penicillin/streptomycin in a 5% CO_2 atmosphere at 37 °C. The cells were seeded at a density of 5×10^3 cells/well in a 96 well culture plate. After 24 h, the cells were treated with 5, 10, 30, 50, and 100 $\mu\text{mol/l}$ icaritin and 30 $\mu\text{mol/l}$ icariin dissolved in DMSO (final concentration 0.1%) and control cells were treated with 0.1% DMSO and 1 $\mu\text{mol/l}$ estradiol. Cells treated with icaritin, icariin or DMSO for 24, 48, and 72 h were incubated with 20 μl of 5 mg/ml 3-(4,5-dimethylthiazol-2-yl)-2,5-diphenyl-tetrazolium bromide (MTT) solution for 4 h. Following this, the medium was discarded, and 500 μl DMSO was added. Absorbance at 570 nm was determined with an ELx800 universal microplate reader (Bio-Rad, USA). By MTT method, cell numbers were obtained as absorbance values. The results are expressed as viability compared with that of control cells. Each treatment and time point had three independent plates. The representative data shown in this study were reproducible in three independent experiments.

2.3. The primary culture of rat prostate basal cells and cell growth-inhibition studies

Minced rat ventral prostate was dissociated by collagenase II digestion, suspended in RPMI-1640 containing 10% BSA, and subjected to Percoll centrifugation to separate the epithelial cells from stromal cells. The cells were cultured in RPMI 1640 medium, supplemented with 10% BSA, 1% penicillin/streptomycin in a 5% CO_2 atmosphere at 37 °C. The cells were seeded at a density of 1×10^4 cells/well in a 96 well culture plate. After 24 h, the cells were treated with 5, 10, 30, and 50 $\mu\text{mol/l}$ icaritin dissolved in DMSO (final concentration 0.1%) and control cells were treated with 0.1% DMSO, respectively. MTT method as described above was used to assess cell viability.

2.4. Interaction with ICI 182,780

Some phytoestrogens, such as genistein and daidzein, act both as agonists and antagonists at estrogen receptors. In the

present study, we examined the effects of icariin and icaritin as well as their interaction with ICI 182,780, a pure estrogen receptor antagonist. The concentration of icariin and icaritin was set as detailed above, and the effect of cotreatment with 1 $\mu\text{mol/l}$ ICI 182,780 on cell growth was assessed by the MTT assay method after the desired treatment time as described above.

2.5. Cell cycle analysis by flow cytometry

PC-3 cells were grown in 10% serum condition in the culture medium as mentioned above. At $\sim 30\%$ confluency, cells were treated with DMSO control or 5, 10, 30, and 50 $\mu\text{mol/l}$ icaritin and 30 $\mu\text{mol/l}$ icariin and at the end of desired treatment time (24 and 48 h), cells were harvested and 1×10^6 cells were placed into a polypropylene tube and centrifuged. The supernatant was removed and 1 ml 4 °C 70% ethanol was added dropwise to the cell pellet during vortexing. The cells were kept at 4 °C until DNA staining. Fixed cells were treated with 100 $\mu\text{g/ml}$ RNase A in phosphate-buffered saline solution (PBS) for 1 h, followed by staining with 50 $\mu\text{g/ml}$ propidium iodide in PBS. Flow cytometric analysis of cell cycle distribution and apoptosis was performed with a BD FACSCalibur with a 488-nm (blue) argon laser (Becton Dickinson, San Jose, CA). Data acquisition was performed with CellQuest 3.1 software and data were analyzed with ModFit LT 3.0 software (Variety Software House, Topsham, ME).

2.6. Protein extraction and western blot analysis

The prostate cancer cells were plated and cultured in complete medium and allowed to attach for 24 h followed by the addition of 5, 10, 30, and 50 $\mu\text{mol/l}$ icaritin and 30 $\mu\text{mol/l}$ icariin. Incubation was carried out for 24 and 48 h. Control cells were incubated in the medium with 0.1% DMSO for the same time period. After the indicated period, cells were harvested at 4 °C and lysed on ice in extraction buffer containing Tris-HCl (20 mM, pH 7.5), NaCl (150 mM), EDTA (1 mM), Triton X-100 (1%), sodium deoxycholate (0.5%) plus PMSF (1 mM), leupeptin (10 $\mu\text{g/ml}$), and aprotinin (30 $\mu\text{g/ml}$). Lysates were cleared by centrifugation (4 °C, 14 000 g, 30 min). Total protein present in each lysate was quantified by using a modified Lowry assay (DC protein assay; Bio-Rad, Hercules, USA). Sodium dodecyl sulfate-polyacrylamide gel electrophoresis (SDS-PAGE), Western blotting, and densitometric measurement were performed by standard protocols. Total protein content (40 μg lysate per lane) was analyzed, and the proteins were transferred to a nitrocellulose membrane. Transferred membranes were blocked for 1 h in 5% nonfat milk in Tris-buffered saline containing 0.1% Tween-20 (TBS/T). Primary antibodies were added in 5% milk, and the blot was incubated overnight at 4 °C. The blots were washed three times for 5 min each with 10 ml TBS/T and incubated with secondary antibody (anti-mouse HRP or anti-rabbit HRP, 1:3000; Santa Cruz Biotechnology, USA) in 10 ml TBS/T with gentle agitation for 1 h at room temperature. Then the blots were washed three times for 5 min each with TBS/T, exposed to a chemiluminescent detection system using the SuperSignal West Pico Substrate (Pierce,

Rockford, USA) and exposed to film. Digital images of the films were captured and quantified using the bio-imaging system (Bio-Rad, USA). The expression levels of aimed proteins in treated cultures were compared with those of untreated control cultures.

2.7. Mitochondrial transmembrane potential ($-\Psi_m$) examination

To assess the mitochondrial $\Delta\Psi_m$, 5,5',6,6'-tetrachloro-1,1',3,3'-tetraethylbenzimidazolocarbocyanine iodide (JC-1, Sigma, USA) staining was used. JC-1 is a cationic dye that exhibits potential-dependent accumulation in mitochondria, indicated by a fluorescence emission shift from green (525 ± 10 nm) to red (610 ± 10 nm). Mitochondria depolarization is specifically indicated by a decrease in the red to green fluorescence intensity ratio (Zuliani et al., 2003).

2.8. Fluorescence morphological examination

Cell morphology of icaritin-induced apoptosis was investigated by staining the cells with a combination of the fluorescent DNA-binding dyes acridine orange (AO) and ethidium bromide (EB). Cells were sorted into four groups with dual staining: (a) viable, non-apoptotic (VNA), (b) viable, apoptotic (VA), (c) non-viable, apoptotic (NVA), and (d) non-viable, non-apoptotic (NVNA). Briefly, cells were harvested and washed with PBS after being exposed to different concentrations of icaritin and icariin or DMSO for 48 h and were stained with 100 $\mu\text{g/ml}$ AO/EB for 5 min. Then cells were observed under a fluorescence microscope (Leica) according to their color and structure (Pitrak et al., 1996).

2.9. Statistical analysis

All experiments were repeated thrice. Western blot results were presented from a representative experiment. The number of viable/dying cells or cell colonies in the control group or the initial time point was assigned a relative value of 100%. All data are expressed as means \pm standard deviation (S.D.), and the level of significance between two groups was assessed with Student's *t*-test. *P* values of less than 0.05 were considered to be statistically significant.

3. Results

3.1. Effects of icariin and icaritin on growth of PC-3 and rat prostate basal cells

To assess the biological activity of these compounds in terms of cell growth and death, PC-3 cells were treated with 5, 10, 30, 50, and 100 $\mu\text{mol/l}$ doses of icaritin for 24, 48, and 72 h. Icaritin (30–100 $\mu\text{mol/l}$) showed a strong dose- and time-dependent inhibition of cell growth, accounting for 66.10% to 86.27% ($P < 0.001$), 72.13% to 89.90% ($P < 0.001$), and 73.09% to 88.67% ($P < 0.001$) growth inhibition after 24, 48, and 72 h of treatment, respectively (Fig. 2A and B). However, similar treatment with icariin (30 $\mu\text{mol/l}$ for 24, 48, and 72 h) showed

weak efficacy, accounting for 5.95% ($P>0.05$), 7.73% ($P>0.05$), and 2.48% ($P>0.05$) growth inhibition, respectively (Fig. 2A). Meanwhile, primary cultured rat prostate basal cells treated with icaritin (30–50 $\mu\text{mol/l}$) showed a comparatively weak dose- and time-dependent inhibition of cell growth, accounting for 64.87% to 59.48% ($P>0.05$), 55.79% to 49.98% ($P>0.05$), and 50.98% to 50.82% ($P>0.05$) growth inhibition after 24, 48, and 72 h of treatment, respectively. These data suggest that icaritin is much potent in inhibiting the growth of PC-3 (at 48 h IC_{50} was $10.74 \pm 1.59 \mu\text{mol/l}$, $P<0.001$) as compared with icariin. Meanwhile, icaritin induced a more differentiated, fibroblast-like phenotype in PC-3 cells after longer incubation (48–72 h, Fig. 2C). This effect might be related to the growth-inhibitory

effects of transforming growth factor-beta (TGF-beta), which could generate the occurrence of a more fibroblast-like phenotype. Since transforming growth factor-beta modulates cell cycle progression in different cell types, further examinations will detect how long would PC-3 cells survive in the presence of 30 or 50 $\mu\text{mol/l}$ icaritin, if they would change their phenotype further, and the possible mechanism. Also it would be examined whether withdrawal of icaritin could allow the cells to regain their previous phenotype or whether the changes are permanent. The differences in biological activity of icaritin and icariin could be attributed to the difference in their chemical structures (Fig. 1). PC-3 cancer cell line was more sensitive to icaritin than rat prostate basal cells (Fig. 2D and E).

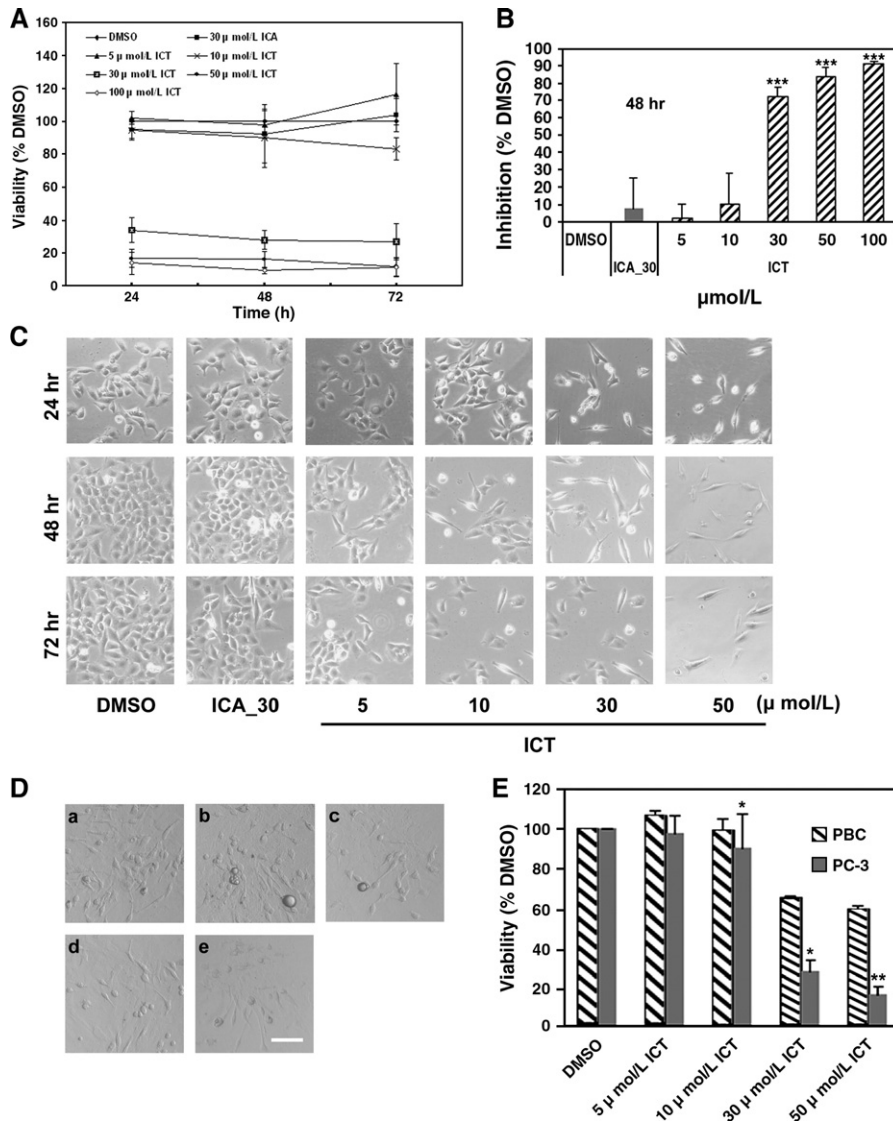


Fig. 2. Inhibitory effects of icaritin and icariin on PC-3 cells growth. (A, B) Selective effects of icaritin and icariin on exponentially growing PC-3 cells, 5×10^3 cell/well were plated in 96 well plates and the next day, cells were treated with either DMSO vehicle control or 5–100 $\mu\text{mol/l}$ icaritin and 30 $\mu\text{mol/l}$ icariin in complete medium. Results were averaged from three independent experiments and presented as means \pm S.D., *** $P<0.001$ versus control. (C) Cell morphology in DMSO, 30 $\mu\text{mol/l}$ ICA and 5–50 $\mu\text{mol/l}$ ICT treated PC-3 cells (magnification 100 \times). (D, E) Effect of icaritin on exponentially growing primary cultured rat prostate basal cells, 1×10^4 cell/well were plated in 96 well plates and the next day, cells were treated with either DMSO vehicle control or 5–50 $\mu\text{mol/l}$ icaritin in complete medium (a–e: treated with DMSO, and 5–50 $\mu\text{mol/l}$ ICT, respectively; magnification 100 \times). Results were averaged from three independent experiments and presented as means \pm S.D., * $P<0.05$, ** $P<0.01$ versus viability of PC-3 cells in the same treatment group. After 24, 48, and 72 h exposure, total cells were treated with MTT for 4 h and cell numbers were harvested as absorbance values. ICA, icariin; ICT, icaritin. PBC, prostate basal cells.

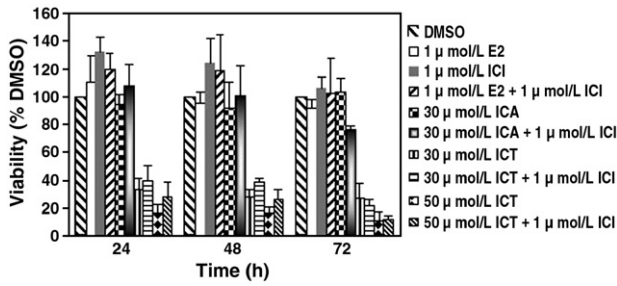


Fig. 3. Effect of cotreatment with pure antiestrogen ICI 182,780 on cell growth inhibition induced by icaritin and icariin in PC-3 cells. 5×10^3 cell/well were plated in 96 well plates and the next day, cells were treated with either DMSO vehicle control or 1 μmol/l estradiol, 30, 50 μmol/l icaritin and 30 μmol/l icariin for 24, 48, and 72 h. Incubation with DMSO alone was performed as control and the final concentration of vehicle, DMSO, in the medium never exceeded 0.1%. After incubation for desired days, the MTT assay was performed to measure cell viability. Results were averaged from three independent experiments and presented as means±S.D.; ICA, icariin; ICT, icaritin; E₂, estradiol; ICI, ICI 182,780.

3.2. Icaritin-induced growth inhibition with no association with estrogen receptors

Then, an experiment was designed to determine whether the growth-inhibiting effect induced by icaritin and icariin could be blocked by ICI 182,780, a specific estrogen receptor antagonist.

Co-incubation with 1 μmol/l ICI 182,780 caused negligible alteration to treatment of 1 μmol/l estradiol, 30, 50 μmol/l icaritin and 30 μmol/l icariin for 24, 48, and 72 h (Fig. 3). Thus, inhibition of cell proliferation could not be associated with estrogen receptors, but might be the result of the induction of apoptosis or cell cycle growth arrest. We hypothesized that icaritin-induced inhibition of cell proliferation was due to alterations in cell cycle control and programmed cell death.

3.3. Icaritin induced a strong G₁ arrest in cell cycle progression of prostate cancer cells

Inhibition of deregulated cell cycle progression in cancer cells is an effective strategy to halt tumor growth (Noble et al., 2005). Because we observed a strong growth-inhibitory effect of icaritin, we then analyzed its possible inhibitory effect on cell cycle progression following 5, 10, 30, and 50 μmol/l doses of icaritin treatment for 48 h. We observed that icaritin (5, 10, and 30 μmol/l) induced G₁ arrest after the treatment in PC-3 cells (Fig. 4A). An optimum dose-dependent effect was observed at 48 h of treatment where icaritin caused 59.35±6.80%, 63.42±6.18%, and 77.05±8.08% ($P < 0.05$) PC-3 cells in G₁ phase as compared with 55.81% in control (Fig. 4B). An increase in G₁ cell population was mostly at the expense of S phase cells ($P < 0.01$) with a minimal decrease in G₂-M cell population

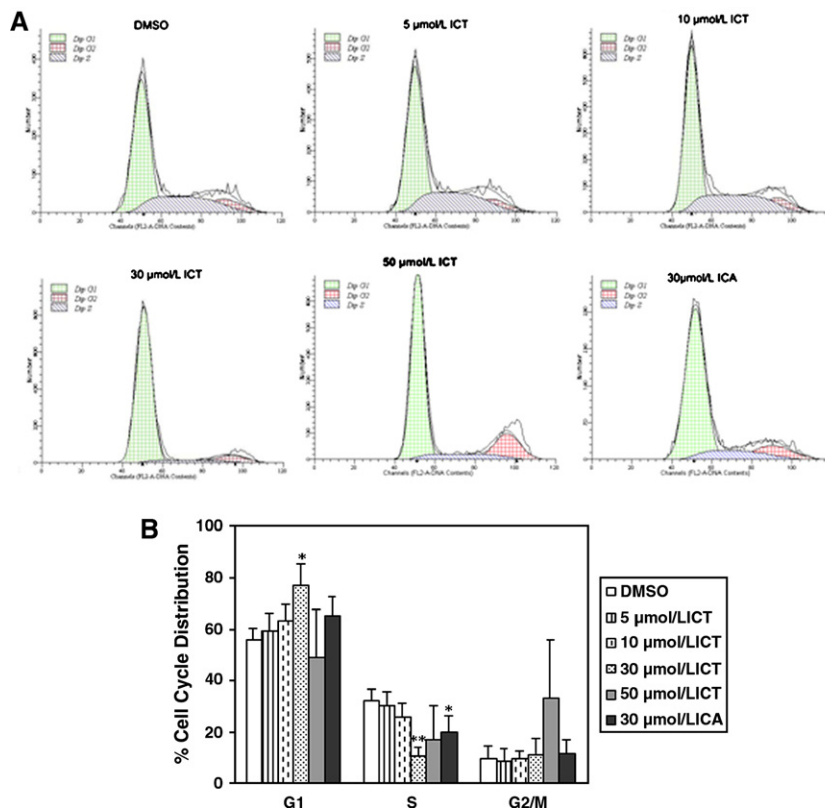


Fig. 4. Effect of icariin and icaritin on cell cycle progression in PC-3 cells. Cells were cultured in complete medium, and treated with either DMSO vehicle control or 30 μmol/l icariin and 5–50 μmol/l icaritin. After 48 h of these treatments, cells were collected, washed with PBS, digested with RNase, and then cellular DNA was stained with propidium iodide as detailed in Materials and methods. Flow cytometric analysis was then performed for cell cycle distribution. (A) Propidium iodide fluorescence pattern for cell cycle distribution in different treatment. (B) The percentage of cell cycle distribution for each treatment group. Mean±S.D. of three independent samples. ICA, icariin; ICT, icaritin; * $P < 0.05$; ** $P < 0.01$ versus control.

(Fig. 4B). 50 $\mu\text{mol/l}$ icaritin induced a medium increase in G₂-M cell population (Fig. 4A and B). 48 h treatment of 30 $\mu\text{mol/l}$ icaritin showed only weak G₁ arrest 65.37 \pm 7.08% ($P>0.05$). We then investigated whether G₁ cell cycle regulatory molecules were altered in icaritin treated PC-3 cells.

3.4. Icaritin-mediated alterations in expression of phosphorylated pRb, pRb, Cyclin D1 and CDK4 complexes, p27^{Kip1}, and p16^{Ink4a}

Since, we observed optimum G₁ cell cycle arrest by icaritin at 48 h in PC-3 cells, and a relatively similar effect at 24 h (data not shown); we investigated whether G₁ cell cycle regulatory molecules are altered in icaritin treated PC-3 cells. Total cell lysates were prepared following icaritin treatment of cells at 5, 10, 30 doses and icaritin treatment of cells at 30 $\mu\text{mol/l}$ dose for 24 and 48 h, and 50 $\mu\text{mol/l}$ icaritin at 48 h. Western blot analysis of total cell lysates (40 $\mu\text{g/sample}$) showed a strong dose- and

time-dependent increase in the expression of p27^{Kip1} and p16^{Ink4a} from 0 to 30 $\mu\text{mol/l}$ icaritin (Fig. 5A), and no alteration of these expression between 0 and 50 $\mu\text{mol/l}$ icaritin (data not shown). Reprobing of membranes for β -actin confirmed equal protein loading (Fig. 5A and B, bottom). The induction both of p27^{Kip1} and p16^{Ink4a} protein expression was generally associated with the inhibition of cell growth, as they have been demonstrated to be cyclin-dependent kinase inhibitors (Ricardo et al., 1999; Sharpless and DePinho, 1999).

Furthermore, we investigated the protein expression level of a cyclin-dependent protein kinase, CDK4, which interacts with D type cyclins and facilitates the progression of cells through G₁ cell cycle phase (Marcos and Mariano, 2005). In the studies analyzing its effect on the level of CDK4 and cyclin D1 associated with G₁ phase, icaritin treatment for 24 and 48 h showed a dose-dependent decrease in the expression of these proteins (Fig. 5A and B) except an obvious increase of Cyclin D1 at 50 $\mu\text{mol/l}$ treatment (Fig. 5B).

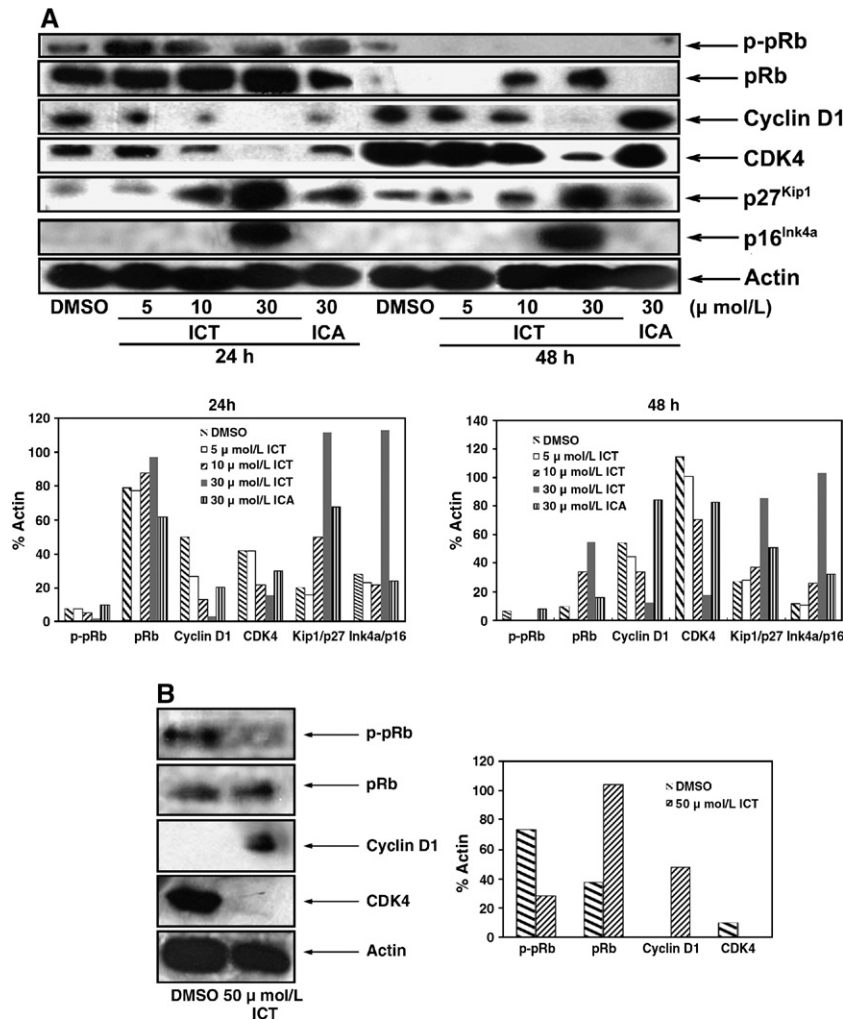


Fig. 5. Effect of icaritin and icaritin on G₁ cell cycle regulators in PC-3 cells. (A) Cells were cultured in complete medium, and treated with either with DMSO vehicle control or 30 $\mu\text{mol/l}$ icaritin and 5, 10, 30 $\mu\text{mol/l}$ icaritin as described in Materials and methods. (B) Cells were cultured in complete medium, and treated with 50 $\mu\text{mol/l}$ icaritin for 48 h. At the end of treatments, total cell lysates were prepared and subjected to SDS-PAGE followed by Western immunoblotting. Membranes were probed with anti-phosphorylated pRb (p-pRb), pRb, Cyclin D1, CDK4, p27^{Kip1}, p16^{Ink4a} and β -actin antibodies followed by peroxidase-conjugated appropriate secondary antibodies, and visualized by enhanced chemiluminescence detection system. Experiments were repeated three times, and share the similar results, a representative blot is shown for each protein. ICA, icaritin; ICT, icaritin.

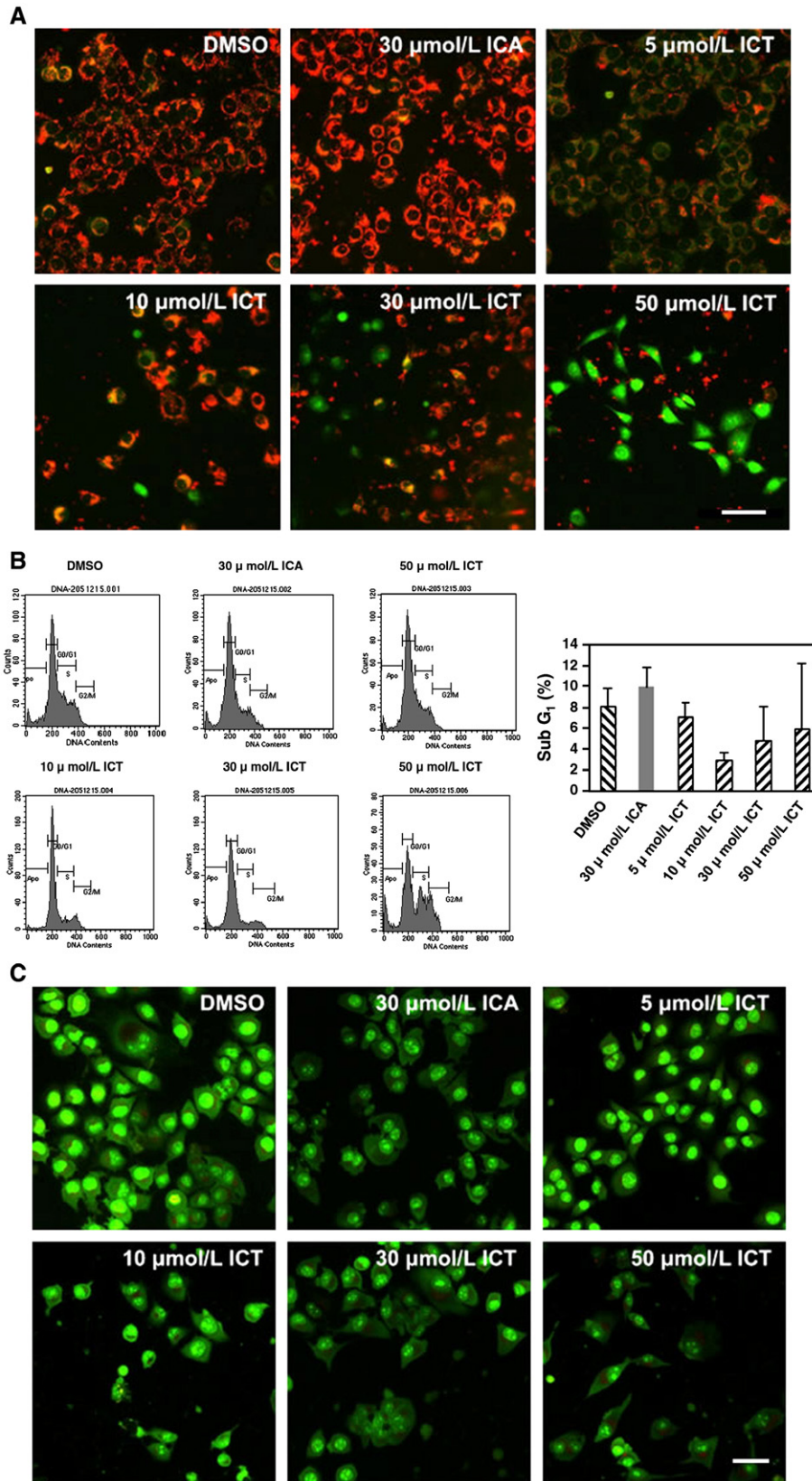


Fig. 6. Effect of icaritin and icariin on mitochondrial transmembrane potential, sun-G₁ cell subpopulation and morphology in PC-3 cells. (A) After cultured in complete medium, and treated with either DMSO vehicle control or 30 μmol/l icariin and 5–50 μmol/l icaritin as described in Materials and methods, PC-3 cells were incubated with JC-1 (0.3 μg/ml) for 15 min at 37 °C. Pictures were taken under a fluorescent microscope (magnification 100×). (B) Propidium iodide fluorescence pattern for sun-G₁ cell subpopulation in different treatment. The experiments were repeated thrice with similar results and a representative illustration is shown for each treatment. Apo, apoptosis. (C) Identification of apoptotic cells using acridine orange-ethidium bromide staining in different treatment (magnification 100×).

Collectively, these results indicated a novel mechanism of icaritin-induced G₁ cell cycle arrest in PC-3 cells. We further sought to investigate whether additional molecular mechanism (s) exists by which icaritin inhibits G₁ cell cycle arrest and studied the Retinoblastoma protein (pRb), which is a central molecule in G₁ cell cycle control, and accordingly, its product (p-pRb). During the progression of G₁ phase and entering into S phase, the pRb is hyperphosphorylated by early and late G₁ phase specific cyclin-dependent kinases and releases E2F transcription factors which, in turn, activates S phase specific genes and help progress cells enter into S phase (Liang, 2005). Icaritin treatment showed a dose-dependent increase of pRb, and that this effect was more pronounced at 10–30 $\mu\text{mol/l}$ concentration within 48 h of treatment (Fig. 5A) while 50 $\mu\text{mol/l}$ icaritin showed a median increase of pRb (Fig. 5B) and 30 $\mu\text{mol/l}$ icaritin exhibited a few decrease (Fig. 5A). On the other hand, a dose-dependent decrease of phosphorylated pRb has exhibited from 0–50 $\mu\text{mol/l}$ icaritin, while 30 $\mu\text{mol/l}$ icaritin showed a weak decrease (Fig. 5A, B).

3.5. Icaritin-induced drop in mitochondrial transmembrane potential at early stage treatment on PC-3 cells

In addition to cell cycle arrest, the growth inhibition induced by icaritin treatment could also be due to programmed cell death; hence, we investigated whether icaritin-induces apoptosis.

Since the loss of mitochondrial transmembrane potential ($-\Psi\text{m}$) is a hallmark for apoptosis, we investigated this potential level in PC-3 cells using JC-1 dye. In non-apoptotic cells, JC-1 accumulates as aggregates in the mitochondria which stain red. Whereas, in apoptotic and necrotic cells, JC-1 exists in monomeric form and stains the cytosol green. The red/green ratio is an indicator of $-\Psi\text{m}$, which is independent of dye-loading, lightscattering, and other optical factors (Szilagyi et al., 2006). After 24 h treatment, 5–50 $\mu\text{mol/l}$ icaritin lowered mitochondrial transmembrane potential presented as green fluorescence in a dose-dependent manner, while 0 $\mu\text{mol/l}$ icaritin and 30 $\mu\text{mol/l}$ icaritin treatment caused no alteration and emitted strong red fluorescence mostly in cytosol (Fig. 6A), indicating a dose-dependent depolarization of the mitochondrial transmembrane, which might be associated with cell apoptosis or necrosis, induced by 5–50 $\mu\text{mol/l}$ icaritin within 24 h treatment (Huang et al., 2004; Bedner et al., 1999).

Then flow cytometric analysis was employed to verify the occurrence of apoptosis. Flow cytometric analysis of cells with sub-G₁ DNA content following staining with propidium iodide is a widely accepted technique for apoptosis detection. However, exposure of PC-3 cells to icaritin and icaritin for 48 h showed only very slight increase of sub-G₁ cell subpopulation and did not affect it significantly (Fig. 6B). This flow cytometry analysis demonstrated that there were few cells that went apoptosis in each treatment group.

On the other hand, we used AO-EB dyes to investigate cell morphology. After 48 h treatment, a number of cells exhibited a flattened polygonal morphology, whereas few cells showed morphological features of apoptosis (membrane broken, and breaking up of the nuclei) or revealed any orange stain that is

typical for necrosis, though there is a significant decrease in cell volume (Fig. 6C). AO-EB staining demonstrated that few morphological alterations could be found even after 48 h icaritin treatment. All of these results indicated that icaritin-induced early stage dose-dependent depolarization of the mitochondrial transmembrane followed markedly with neither apoptosis nor necrosis after 48 h icaritin treatment (later stage).

4. Discussion

The central and novel finding in the present study is the identification of *in vitro* anticancer efficacy of icaritin against advanced human prostate carcinoma PC-3 cells. The completed studies clearly and convincingly showed that icaritin caused a G₁ cell cycle arrest via an induction of p27^{Kip1} and to a lesser extent p16^{Ink4a} together with an inhibition in CDK4-cyclin D1 complex as an underlying mechanism in its PC-3 cell growth inhibition. Furthermore, this agent-caused mitochondrial transmembrane potential ($-\Psi\text{m}$) drop in PC-3 cells.

ICI 182,780 is a specific estrogen receptor antagonist. Here, we observed that icaritin-induced inhibition of PC-3 growth altered little when co-incubated with ICI 182,780, suggesting that estrogenic activity of icaritin had no role in affecting a growth-inhibitory response.

In previous studies, prenylflavonoids have been shown to cause alterations in cell cycle regulation in a number of cell lines (Stevens and Page, 2004). We performed flow cytometry analysis to confirm the alterations in cell cycle regulatory properties of these prenylflavonoids, icaritin and icaritin. Results indicate that icaritin (5–30 $\mu\text{mol/l}$) caused a G₁ arrest in PC-3 cells. The percentage of cells in G₁ phase increased with corresponding decrease in the percentage of cells in the S phase cells. We hypothesized this cell cycle arrest might attribute to G₁ cell cycle regulatory molecules and their expressive alterations.

Cyclin-dependent kinases, cyclin-dependent kinase inhibitors, and cyclins play essential roles in the regulation of cell cycle progression. Cyclin-dependent kinase inhibitors are tumor suppressor proteins that down-regulate the cell cycle progression by binding with active cyclin-dependent kinase-cyclin complexes and thereby inhibiting their kinase activities (Yim et al., 2005). A common characteristic of tumor suppressor genes is their ability to inhibit cell proliferation when over-expressed in sensitive cell lines. The inhibition of cell growth observed in icaritin-treated cells may be due to induction of G₁ cell cycle arrest as a result of multiple gene activities. We found that two important cyclin-dependent kinase inhibitors, p27^{Kip1} and p16^{Ink4a}, were up-regulated in PC-3 cells treated with 5–30 $\mu\text{mol/l}$ icaritin. The p27^{Kip1} is a member of cyclin-dependent kinase inhibitors, which could bind and inhibit a broader range of cyclin-dependent kinases. The expression of p27^{Kip1} has been shown to be up-regulated during TGF- β mediated antiproliferative response, serum starvation or density arrested cells (Polyak et al., 1994; Slingerland et al., 1994). Recent studies have also indicated the prognostic significance of cyclin-dependent kinase inhibitors in prostate cancer. Specifically, p27^{Kip1} expression has been shown to be an independent predictor of prostate-specific antigen failure following radical

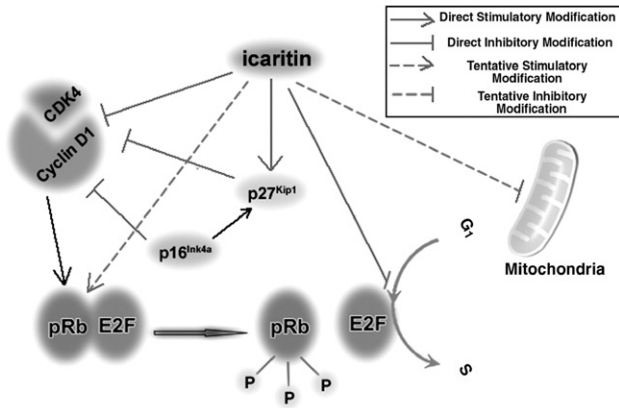


Fig. 7. Inducible effects of icaritin. Icaritin on cell death followed by pRb, p27^{Kip1} and p16^{Ink4a} protein up-expressions and phosphorylated pRb, Cyclin D1 and CDK4 protein down-expressions in PC-3 cells. Induction of the cell cycle regulatory pathways contributed to the inactivation of E2F, which plays an important role in entering from G₁ to S. Meanwhile, icaritin also caused drop of mitochondrial transmembrane potential, which often exists in early strategy of apoptosis. Both mechanisms could due to the cell growth inhibition of PC-3 cells.

prostatectomy, and its low expression is correlated with poor disease-free survival in prostate cancer patient (Yang et al., 1998; Freedland et al., 2003). Therefore, the up-regulation of p27^{Kip1} may be an important molecular mechanism through which icaritin inhibits cancer cell growth.

The increased expression of G₁ cyclin, Cyclin D1, in cancer cells provided them an uncontrolled growth advantage because most of these cells either lack cyclin-dependent kinase inhibitors, harbor nonfunctional cyclin-dependent kinase inhibitors, or cyclin-dependent kinase inhibitors expression is not at a sufficient level to control cyclin-dependent kinase activity (Dulic et al., 1992). Consistent with these reports, cell cycle analysis data showed that icaritin (5–30 μmol/l) caused a dose-dependent G₁ arrest in cell cycle progression of prostate cancer cells, and the growth-inhibitory effect of icaritin could also be directly related to its ability to down-regulate CDK4, which is one of the critical molecules required for early progression of the G₁ cell cycle.

Binding of p16^{Ink4a} to CDK4 prevents association of CDK4 with the D-type cyclins and results in an inhibition of the catalytic activity of the cyclin D/CDK4 enzymes. Thus, overexpression of p16^{Ink4a} in PC-3 cells might due to an arrest in the G₁ phase of the cell cycle.

In vitro, complexes of cyclin D1 and CDK4 can phosphorylate the product of the retinoblastoma tumor suppressor gene, pRb. The phosphorylation of pRb, occurring in mid/late G₁, reverses its growth-inhibitory effect and enables cells to proceed from G₁ to S phase. The timing of cyclin D-dependent kinase activity and the onset of pRb hyperphosphorylation appear to coincide in the cell cycle. Taken together, these findings suggest that cyclin D/CDK complexes play a critical role in pRb hyperphosphorylation *in vivo*. Consistent with these, our data showed that icaritin (5–30 μmol/l) increased the expression of pRb and decreased phosphorylated pRb in a dose- and time-dependent manner (Fig. 7).

Previous studies have demonstrated that, p16^{Ink4a} could negatively regulate cell proliferation by suppressing hyperphosphorylation and functional inactivation of pRb. In contrast, cells that lack functional pRb appear not to be affected by high levels of p16^{Ink4a}, demonstrating that pRb mediates the growth suppression by p16^{Ink4a}. Since p16^{Ink4a} has been shown to specifically inhibit cyclin D1/CDK4 complexes, these findings indicate that pRb is the critical target of these complexes in order to promote progression through the G₁ phase of the cell cycle. The evidence presented here connects two tumor suppressors, p16^{Ink4a} and pRb, in one pathway controlling cell growth. In this pathway cyclin D/CDK complexes would mediate the inactivation of pRb, either directly or indirectly (Rene' et al., 1995). Several lines of evidence suggest that inactivation of this growth-regulatory pathway might be an absolute requirement for the progression of certain tumors. Thus, results came from our experiment showed that icaritin (5–30 μmol/l) could both up-regulate the expression of p27^{Kip1}, p16^{Ink4a} together with pRb and down-regulate the expression of phosphorylated pRb, cyclin D1 and CDK4. In other words, icaritin could inhibit PC-3 cell growth by regulating every stage through the cyclin D1-CDK4-p16^{Ink4a} pathway (Ortega et al., 2002; Semczuk and Jakowicki, 2004).

Furthermore, we also observed that 50 μmol/l icaritin reduces G₂-M arrest at the expense of G₁ phase cell population. This suggests that, at this dose, the mechanism of action of icaritin differs from the action of lower doses. Treatment with this concentration of icaritin unexpectedly increased expression of Cyclin D1 but caused similar changes in pRb, phosphorylated pRb, and CDK4 expression as 30 μmol/l icaritin.

Most of the presently available cytotoxic anticancer drugs mediate their effect *via* apoptosis induction in cancer cells, and apoptosis is suggested as one of the major mechanisms for the targeted therapy of various cancers including prostate cancer. In case of advanced prostate cancer, cancer cells become resistant to apoptosis and do not respond to cytotoxic chemotherapeutic agents (Yim et al., 2005). Therefore, the agents that induce apoptotic death of hormone-refractory prostate cancer cells could be useful in controlling this malignancy. Consistent with this approach, our data showing an induction of apoptotic death of advanced prostate cancer cells by icaritin could be of a significance in identifying another anticancer mechanism (together with a greater significance of cell cycle arrest) of icaritin for its possible application in prostate cancer control. Because induction of cyclin-dependent kinase inhibitors has been reported in anticancer agent-caused apoptosis in human prostate cancer cells (Don et al., 2001), the icaritin-induced cyclin-dependent kinase inhibitors could be, in part, responsible for the observed apoptotic death of PC-3 cells.

JC-1 is a non-toxic fluorescence probe to monitor membrane potential. This dye has no effect on living cells, including their respiration. JC-1 monomers accumulate selectively in mitochondria and subsequently aggregate as a consequence of the membrane potential. This reaction is pH independent within the physiological range. The electrochemical gradient is responsible for this J aggregation. The change in binding of JC-1 is

manifested by a loss of red fluorescence, which represents the aggregate binding of this dye in mitochondria. On the other hand, the mitochondrial transmembrane potential decreases early during apoptosis (Huang et al., 2004; Bedner et al., 1999). Thus, we demonstrated that early stage of icaritin treatment (5–50 $\mu\text{mol/l}$ for 24 h) induced dose-dependent depolarization of the mitochondrial transmembrane might be associated with cell apoptosis or necrosis, while 30 $\mu\text{mol/l}$ icaritin treatment has no activity of inducing apoptosis.

However, after 48 h treatment, these apoptotic or necrotic signals diminished, for the results of flow cytometry analysis showed that, the percentage of apoptosis cells of icaritin (5–50 $\mu\text{mol/l}$) treatment group is similar to that of DMSO treatment group. Flow cytometry techniques that are widely used in studies of cell death, and particularly in the identification of apoptotic cells, generally rely on the measurement of a single characteristic biochemical or molecular attribute (Bedner et al., 1999). However, these methods fail to recognize cell death lacking that attribute, as in some examples of atypical apoptosis. Since apoptosis was originally defined by morphologic criteria, and mitochondrial metabolism is closely linked to mechanisms regulating apoptosis, we let the cytometry defined apoptosis be confirmed by morphologic examination.

Thus, we used AO-EB staining, which allows the identification of viable, apoptotic and necrotic cells based on color and appearance (Gao et al., 2005). Viable cells were green with intact nuclei. Non-viable cells had bright orange chromatin. Apoptosis was demonstrated by the appearance of cell shrinkage with condensation and breaking up of the nuclei. Thus, apoptotic cells were easily distinguished from necrotic cells because the latter appeared orange with a normal nuclear structure. Herein, little morphological changes could be detected in icaritin treated cells by using AO-EB staining. Cells undergo death by two major mechanisms: necrosis, in which primary damage to the metabolic or membrane integrity of the cell occurs; and apoptosis, which is an internal suicide programme contained in all cells. Taken together, we concluded that, icaritin principally caused cell death by cell cycle arrest in the entire process, and induced depolarization of the mitochondrial transmembrane, which might be associated with cell apoptosis or necrosis, in early treatment stage. However, a detailed molecular mechanism is far from clear and requires further exploration.

In conclusion, the results of our studies provide experimental evidence that icaritin inhibited cell growth of PC-3 prostate cancer cells, arrested cell cycle with alterations in phosphorylated pRb, pRb, cyclin D1, CDK4, p27^{Kip1}, and p16^{Ink4a} protein expression but not associated with estrogen receptors, and decreased mitochondrial transmembrane potential in early stage treatments. The nature of icaritin in selectively mediating the above mentioned responses in PC-3 cells, in conjunction with its nontoxic nature, could make it a potentially effective chemopreventive or therapeutic agent against prostate cancer. However, further *in vivo* studies are needed to establish the role of icaritin as a chemopreventive or therapeutic agent against prostate cancer.

Acknowledgements

This work was funded by the National Natural Science Foundation of China and we sincerely thank the Foundation for its support. We also sincerely thank Mr. Zhiqiang Wang for his work of purification of icaritin.

References

- Bedner, E., Li, X., Gorczyca, W., Melamed, M.R., Darzynkiewicz, Z., 1999. Analysis of apoptosis by laser scanning cytometry. *Cytometry* 35, 181–195.
- Colgate, E.C., Miranda, C.L., Stevens, J.F., Bray, T.M., Ho, E., 2006. Xanthohumol, a prenylflavonoid derived from hops induces apoptosis and inhibits NF-kappaB activation in prostate epithelial cells. *Cancer Lett.* 246, 201–209.
- Don, M.J., Chang, Y.H., Chen, K.K., Ho, L.K., Chau, Y.P., 2001. Induction of CDK inhibitors (p21(WAF1) and p27(Kip1)) and Bak in the beta-lapachone-induced apoptosis of human prostate cancer cells. *Mol. Pharmacol.* 59, 784–794.
- Dulic, V., Lees, E., Reed, S.I., 1992. Association of human cyclin E with a periodic G1-S phase protein kinase. *Science* 257, 1958–1961.
- Freedland, S.J., deGregorio, F., Sacoolidge, J.C., Elshimali, Y.I., Csathy, G.S., Dorey, F., Reiter, R.E., Aronson, W.J., 2003. Preoperative p27 status is an independent predictor of prostate specific antigen failure following radical prostatectomy. *J. Urol.* 169, 1325–1330.
- Gao, L., Shan, B.E., Chen, J., Liu, J.H., Song, D.X., Zhu, B.C., 2005. Effects of spider *Macrochele raven* venom on cell proliferation and cytotoxicity in HeLa cells. *Acta Pharmacol. Sin.* 26, 369–376.
- Greenlee, R.T., Hill-Harmon, M.B., Murray, T., Thun, M., 2001. Cancer statistics, 2001. *CA Cancer J. Clin.* 51, 15–36.
- Huang, Y.T., Chueh, S.C., Teng, C.M., Guh, J.H., 2004. Investigation of ouabain-induced anticancer effect in human androgen-independent prostate cancer PC-3 cells. *Biochem. Pharmacol.* 67, 727–733.
- Liang, Z., 2005. Tumour suppressor retinoblastoma protein Rb: a transcriptional regulator. *Eur. J. Cancer* 41, 2415–2427.
- Linja, M.J., Savinainen, K.J., Tammela, T.L., Isola, J.J., Visakorpi, T., 2003. Expression of ER α and ER β in prostate cancer. *Prostate* 55, 180–186.
- Liu, J., Lou, Y.J., 2004. Determination of icaritin and metabolites in rat serum by capillary zone electrophoresis: rat pharmacokinetic studies after administration of icaritin. *J. Pharm. Biomed. Anal.* 36, 365–370.
- Marcos, M., Mariano, B., 2005. Mammalian cyclin-dependent kinases. *Trends Biochem. Sci.* 30, 630–641.
- Noble, M., Barrett, P., Endicott, J., Johnson, L., McDonnell, J., Robertson, G., Zawaira, A., 2005. Exploiting structural principles to design cyclin-dependent kinase inhibitors. *Biochim. Biophys. Acta* 1754, 58–64.
- Ortega, S., Malumbres, M., Barbacid, M., 2002. Cyclin D-dependent kinases, INK4 inhibitors and cancer. *Biochim. Biophys. Acta* 1602, 73–87.
- Pitrak, D.L., Tsai, H.C., Mullane, K.M., Sutton, S.H., Stevens, P., 1996. Accelerated neutrophil apoptosis in the acquired immunodeficiency syndrome. *J. Clin. Invest.* 98, 2714–2719.
- Polyak, K., Kato, J.Y., Solomon, M.J., Sherr, C.J., Massague, J., Roberts, J.M., Koff, A., 1994. p27Kip1, a cyclin-Cdk inhibitor, links transforming growth factor-beta and contact inhibition to cell cycle arrest. *Genes Dev.* 8, 9–22.
- Rene, H.M., Rafael, E.H., Felix, L., Robert, A.W., 1995. Growth suppression by p16^{Ink4a} requires functional retinoblastoma protein. *Cell Biol.* 92, 6289–6293.
- Ricardo, V.L., Lori, A.E., Long, J., Elzbieta, K., Xiang, Q., John, C.C., 1999. p27^{Kip1}: a multifunctional cyclin-dependent kinase inhibitor with prognostic significance in human cancers. *Am. J. Pathol.* 154, 313–323.
- Santti, R., Makela, S., Strauss, L., Korkman, J., Kostian, M.L., 1998. Phytoestrogens: potential endocrine disruptors in males. *Toxicol. Ind. Health* 14, 223–237.
- Semczuk, A., Jakowicki, J.A., 2004. Alterations of pRb1-cyclin D1-cdk4/6-p16 (INK4A) pathway in endometrial carcinogenesis. *Cancer Lett.* 203, 1–12.
- Sharpless, N.E., DePinho, R.A., 1999. The *INK4A/ARF* locus and its two gene products. *Curr. Opin. Genet. Dev.* 9, 22–30.

- Sim, H.G., Cheng, C.W., 2005. Changing demography of prostate cancer in Asia. *Eur. J. Cancer* 41, 834–845.
- Slingerland, J.M., Hengst, L., Pan, C.H., Alexander, D., Stampfer, M.R., Reed, S.I., 1994. A novel inhibitor of cyclin-Cdk activity detected in transforming growth factor beta-arrested epithelial cells. *Mol. Cell. Biol.* 14, 3683–3694.
- Stevens, J.F., Page, J.E., 2004. Xanthohumol and related prenylflavonoids from hops and beer: to your good health! *Phytochemistry* 65, 1317–1330.
- Szilagy, G., Simon, L., Koska, P., Telek, G., Nagy, Z., 2006. Visualization of mitochondrial membrane potential and reactive oxygen species via double staining. *Neurosci. Lett.* 399, 206–209.
- Wang, Z.Q., Lou, Y.J., 2004. Proliferation-stimulating effects of icaritin and desmethylcaritin in MCF-7 cells. *Eur. J. Pharmacol.* 504, 147–153.
- Wang, Z.Q., Nadine, W., Lou, Y.J., Peter, P., 2006. Prenylflavonoids as nonsteroidal phytoestrogens and related structure–activity relationships. *ChemMedChem* 1, 482–488.
- Yang, R.M., Naitoh, J., Murphy, M., Wang, H.J., Phillipson, J., deKernion, J.B., Loda, M., Reiter, R.E., 1998. Low p27 expression predicts poor disease-free survival in patients with prostate cancer. *J. Urol.* 159, 941–945.
- Ye, H.Y., Lou, Y.J., 2005. Estrogenic effects of two derivatives of icariin on human breast cancer MCF-7 cells. *Phytomedicine* 12, 735–741.
- Yim, D., Singh, R.P., Agarwal, C., Lee, S., Chi, H., Agarwal, R., 2005. A novel anticancer agent, decursin, induces G1 arrest and apoptosis in human prostate carcinoma cells. *Cancer Res.* 65, 1035–1044.
- Zhao, Y., Cui, Z., Zhang, L., 1997. Effects of icariin on the differentiation of HL-60 cells. *Zhonghua Zhong Liu Za Zhi* 19, 53–55.
- Zuliani, T., Duval, R., Jayat, C., Schnébert, S., André, P., Dumas, M., Ratinaud, M., 2003. Sensitive and reliable JC-1 and TOTO-3 double staining to assess mitochondrial transmembrane potential and plasma membrane integrity: interest for cell death investigations. *Cytometry* 54A, 100–108.

Further reading

- Lloyd, R.V., Erickson, L.A., Jin, L., Kulig, E., Qian, X., Cheville, J.C., Scheithauer, B.W., 1999. p27^{kip1}: a multifunctional cyclin-dependent kinase inhibitor with prognostic significance in human cancers. *Am. J. Pathol.* 154, 313–323.